Using Pump−Probe Fluorescence Depletion To Study the Rotationally Resolved Spectra and the *J*-Dependent Predissociation Rate of CS_2

Huei Tarng Liou,* Yih Chung Chang, Kuang Lang Huang, and Wei Cherng Lin

Institute of Atomic and Molecular Sciences, Academia Sinica, P.O. Box 23-166 Taipei, Taiwan

Received: January 28, 1997; In Final Form: May 7, 1997[⊗]

By monitoring single vibronic level pump−probe fluorescence depletion, the rotationally resolved spectra of the 46 482 cm^{-1} band of CS_2 were recorded. The molecular constants are $\nu_0 = 46\,481.51(11)$ cm^{-1}, $B = 0.098\,09(24)$ cm^{-1}, and $D = 6.7(9.3) \times 10^{-8}$ cm^{-1}. The *J*-dependent predissociation rate was analyzed. At low *J* levels the predissociation rate is dominated by the energy separation and the coupling between the bound and the repulsive states, while at high *J* levels the rate is controlled by the tunneling through the barrier of the centrifugal potential.

I. Introduction

Studies of the spectroscopy of CS_2 below the dissociation limit (278 nm) have been reported by many researches,[1,2,3] but there are only a few attempts on the predissociative state at 210 nm.[4−13] The transition broadening due to the predissociation and to the overlap of the transitions of the dissociation products CS contained in the spectra are the main difficulties that prevented further investigation.[12] By monitoring single vibronic level pump−probe fluorescence depletion, we have recorded the rotationally resolved spectra of CS_2. The entire range of the spectrum was scanned 160 nm wide to cover the region of the predissociation. Among many observed bands, the band at 46 482 cm^{-1} is particularly interesting. The energy of this band is in the range of the $^1B_2(^1\Sigma_u^+)$ electronic state of CS_2.[7] Unlike the other bands, where only P- and R-branches were observed, this is one of the two bands to show a Q-branch feature. It has the slowest predissociation rate among the observed bands. Because the spectra are rotationally resolved, we were able to deduce the predissociation rate of each rotational level from the transition line width. In this study, we report the spectroscopic analysis and *J*-dependent predissociation rate of the band at 46 482 cm^{-1}.

II. Experimental Section

As depicted in Figure 1, one excimer laser (Lambda Physik Lp 200ic) was used to pump two dye lasers (FL3002E) of 0.2 cm^{-1} line width simultaneously. The first dye laser excites the molecule from the (0 0 0) electronic ground state $X^1\Sigma_g^+$ to a rotationally resolved level of the intermediate state (0 10 0) R^3B_2.[2] This is followed by the second dye laser to probe the predissociative state in the neighborhood of 210 nm.

The experimental setup is the same as commonly used in the pump−probe two-color experiment except that the fluorescence from the (0 10 0) R^3B_2 to the (0 16 0) $X^1\Sigma_g^+$ transition of CS_2[14,15] was selectively monitored using a $^1/_8$ m monochromator (Oriel 77250) with resolution of 2−3 nm to avoid CS contamination. For the *J* levels from $J = 3$ to 19, the spectra were recorded with the molecular beam configuration;[12] experiment on remaining high *J* levels up to $J = 49$ were carried out at room temperature with a CS_2 pressure of 60 m Torr.

In this experiment the characteristics of the dye laser were monitored by two unbroadened spectra. These are (1) the I_2 spectra simultaneously were recorded for the purpose of wavelength calibration and (2) the 1−1 transitions appear at the right side of 1+1 transitions.

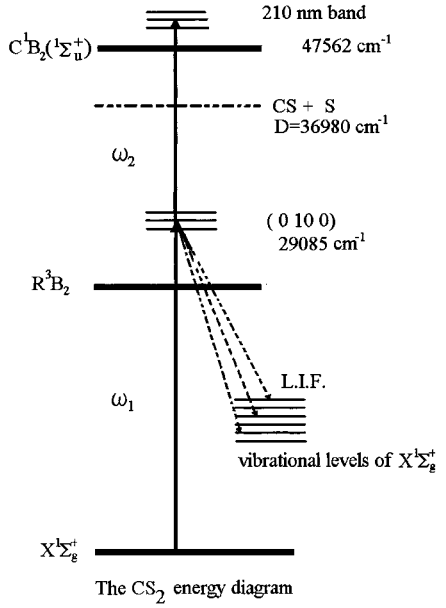

Figure 1. The energy diagram of CS_2 for the pump−probe fluorescence depletion measurement. The frequency ω_1 was fixed, while the ω_2 was scanned. The fluorescence from the (0 10 0) R^3B_2 to (0 16 0) $X^1\Sigma_g^+$ at wavelength 499 nm was monitored.

III. Results and Discussions

A. The Energy Level. As depicted in Figure 2, three kinds of fluorescence depletion result from the scan of the probe laser when the pump laser excites the molecule to a particular *J* level of the intermediate state at the fixed frequency. The first is a continuous background which accounts for about 20% of the depletion. On the top of the continuous background are transitions with broad and narrow linewidths. The fluorescence depletion is caused by the population of the intermediate state being decreased by the probe laser. The transitions with narrow line width are 1−1 multiphoton downward transitions. From our previous stimulated emission pumping studies,[16] these are the (0 10 0) R^3B_2 to (4 22° 0) $X^1\Sigma_g^+$ transitions. The continuous background and the transitions with broad line width are 1+1 multiphoton upward transitions to the upper repulsive dissociation state and the predissociative state, respectively. We

* To whom all the correspondence should be addressed: Fax, 011 886 2 3620501; E-mail, htliou@po.iams.sinica.edu.tw.

⊗ Abstract published in *Advance ACS Abstracts,* July 1, 1997.

S1089-5639(97)00361-7 CCC: $14.00

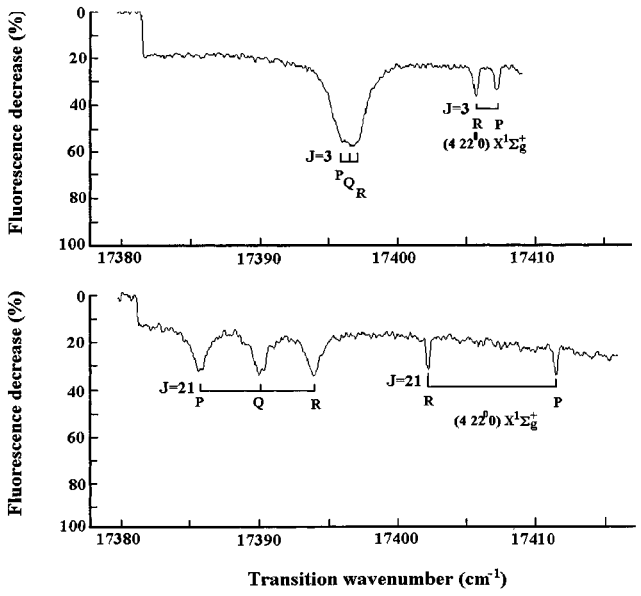

Figure 2. The fluorescence depletion spectra of the 46 482 band of $^1B_2(^1\Sigma_u^+)$, and the (4 22° 0) band of $X^1\Sigma_g^+$. The fluorescence monitored intermediate state is the (0 10 0) R^3B_2 state. The energy level of the intermediate state for $J = 3$ is 29 086.339 cm^{-1}, and for $J = 21$ is 29 137.023 cm^{-1}.

have observed these features in the energy range from 45 100 to 50 600 cm^{-1}. The line width of the predissociative transitions varies from 1.2 to 31 cm^{-1}. The predissociative band, origin at 46 482 cm^{-1}, shown in Figure 2, is particularly interesting because it has the slowest predissociation rate and shows a Q-branch clearly. In the absorption spectrum there is a band head at 46 484.7 cm^{-1}, which was assigned as a hot band $v'' = 3$, $\Delta k = 3$ and denoted as Φ_3^g.[7] In our experiment, due to the pump−probe scheme, the observed band at 46 482 cm^{-1} cannot be a hot band. This may be a 1+1 two-photon resonant band so as to have a symmetry to exhibit a Q-branch. But it raises a question why only two bands with Q-branches were observed in the entire scan. Thus, it is tentatively called the 46 482 cm^{-1} band. As shown in Figure 2, the transition is rotationally resolved at high J levels because only one rotational level of the predissociative state was selectively probed by the selection rule of $\Delta J = 0, \pm 1$ in the intermediate state preparation. Including $J = 3$ and $J = 21$, the spectrum of $J = 5-49$ was recorded one by one. The spectra of $J = 3$ and $J = 45$ were excluded from further analysis, because the former is not well resolved and the latter has a poor signal to noise ratio. Because the assignment of the J quantum number is evident, the rotational analysis becomes straight forward. The energy of the 46 482 band is simply the sum of the observed transition frequency and the energy of the intermediate state (0 10 0) R^3B_2. The state (0 10 0) R^3B_2 has been previously studied by Liou et al.[17] The molecular constants for this state are $\nu_0 = 29\,085.042$ cm^{-1}, $B = 0.11\,253$ cm^{-1}, and $D = 1.9 \times 10^{-7}$ cm^{-1}. The energy levels of (0 10 0) R^3B_2 together with the P, Q, and R transitions are listed in Table 1. The accuracy limit varies with the signal to noise ratio. The energy with the same J level can be either derived from the P-branch or R-branch. For the low J levels, the difference is within 0.06 cm^{-1}. However, for some of the high J levels 25, 31, 33, 39, 41, and 50 it is within 0.2 cm^{-1}. This difference between the P- and R-branch determination is regarded as the accuracy limit. The energy of each J level is schematically shown in Figure 3. The band origin and the rotational constants for the 46 482 cm^{-1} band were determined by a least-squares fitting to the rotational formula

TABLE 1: Energy Levels of (0 10 0) $^3B_2$ and the Transition Frequencies to the 46 482 cm^{-1} Band of the $^1B_2(^1\Sigma_g^+)$ state

J^a	(0 10 0)	P transition	Q transition	R transition	width[b]	error
5	29 088.331	17 395.135	17 396.191	17 397.316	1.486	0.04
7	29 091.29	17 394.295	17 395.704	17 397.297	1.456	0.061
9	29 095.113	17 393.408	17 395.232	17 397.135	1.297	0.066
11	29 099.862	17 392.385	17 394.658	17 396.916	1.442	0.03
13	29 105.483	17 391.257	17 393.929	17 396.521	1.238	0.037
15	29 112.042	17 390.025	17 393.163	17 396.064	1.318	0.063
17	29 119.483	17 388.646	17 392.207	17 395.496	1.202	0.023
19	29 127.813	17 387.129	17 391.151	17 394.771	1.252	0.038
21	29 137.023	17 385.561	17 390.052	17 394.053	1.231	0.03
23	29 147.131	17 383.863	17 388.803	17 393.168	1.115	0.082
25	29 158.127	17 381.973	17 387.504	17 392.073	1.172	0.2
27	29 170.018	17 380.102	17 386.043	17 390.893	1.139	0.081
29	29 182.871	17 378.067	17 384.38	17 389.53	1.363	0.027
31	29 196.549	17 376.024	17 382.691	17 388.166	1.412	0.17
33	29 211.139	17 373.688	17 380.996	17 386.718	1.415	0.11
35	29 226.584	17 371.32	17 379.008	17 385.071	1.366	0.047
37	29 242.945	17 368.742	17 376.942	17 383.265	1.476	0.032
39	29 260.167	17 366.183	17 374.908	17 381.673	1.458	0.14
41	29 278.257	17 363.401	17 372.831	17 379.757	1.543	0.18
43	29 297.285	17 360.664	17 370.581	17 377.7	1.296	0.065
47	29 337.875	17 354.842	17 365.648	17 373.323	1.326	0.03
49	29 359.521	17 351.711	17 363.3	17 371.224	1.241	0.034
51	29 382.062	17 348.558	17 360.287	17 368.601		0.12

[a] The unit is in cm^{-1}. [b] The line width is the fwhm of a Lorentzian profile fitted to the transition line shape. The laser line width has been deconvoluted from a Voigt profile. See the text for more details.

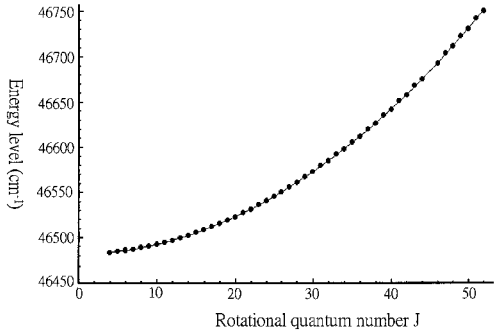

Figure 3. The plot of the energy level of 46 482 band vs rotational quantum number. No apparent perturbation is observed.

$$E = \nu_0 + BJ(J+1) - DJ^2(J+1)^2 \qquad (1)$$

The values derived from all the transitions in the three branches are $\nu_0 = 46\,481.51(11)$ cm^{-1}, $B = 0.098\,09(24)$ cm^{-1}, and $D = 6.7(9.3) \times 10^{-8}$ cm^{-1}. There is a possible reason why the Q-branch was observed in this band. If the molecule at this energy had C_{2v} symmetry, this band would be a perpendicular transition. However, in the neighborhood neither a K-structured band with a Q-branch nor a parallel band with $\Delta K = 0$ was observed to support a C_{2v} symmetry.

B. The *J*-Dependent Predissociation. Figure 4 depicts the relationship between the predissociation rate and the J level schematically. The predissociation rate is derived from $\Delta E/\hbar$, where ΔE is the transition line width listed in Table 1. The line width of each J transition is the fwhm of a Lorentzian profile fitted to the transition line shape, where the line widths of P-, Q-, and R-branches is assumed to be the same value. Using the equation given by Minguzzi et al.,[18] the contribution of the Gaussian line width, which is assumed to be 0.2 cm^{-1}, is deconvoluted from a Voigt profile. The fitting yields a statistical error (one standard deviation) of 0.03 cm^{-1} for the line width. But the accuracy limit for the energy level, the discrepancy in the P and R transition frequency measurement, is taken as the actual accuracy limit for the line width measurement. Intuitively, compared with a data spread of 0.37 cm^{-1} in Figure 4,

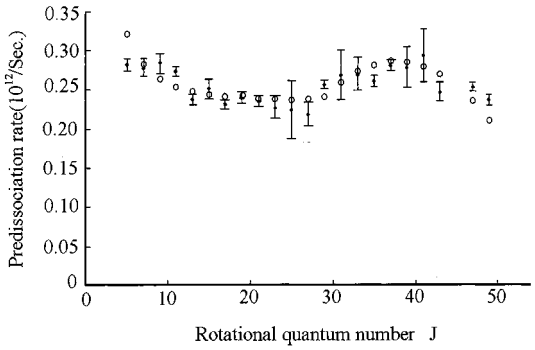

Figure 4. The plot of *J*-dependent predissociation rate of the 46 482 band of CS_2. The solid circles are the experimental values, which were derived from the line width measurement. The error bar for each *J* was derived from the error listed in Table 1. The open circle is the fitting value.

the laser line width of 0.2 cm^{-1} is an important factor for this experiment. However, for example, before deconvoluting from a Voigt profile, the line width for $J = 21$ is 1.254 cm^{-1}, after deconvolution the line width becomes 1.231 cm^{-1}. It indicates that the Gaussian laser line width only contributes less than 2% change to the total line width. The *J*-dependent predissociation rate in Figure 4, first of all, does not show obvious resonance. The plot shows a decreasing trend with a minimum at $J = 27$, then an increasing trend with a maximum at $J = 39$. This is explained by the coupling between the repulsive state and the bound state. The approach of the explanation is as follows.

The observed line width varies with the degree of the couplings between the bound state and the repulsive state. Bound−bound state coupling is disregarded. The reason is that the predissociation rate is on the order of sub-picosecond, which is much faster than a bound−bound state coupling can be. Another reason is that, because the predissociative state is a singlet, no apparent perturbation has been observed in Figure 3. The deduced predissociation rate, *U* is expressed in term of the line width as

$$U = \alpha^2 \frac{\Delta E_r}{\hbar} + \beta^2 \frac{\Delta E_b}{\hbar} \tag{2}$$

$$\psi_a = \alpha\psi_r - \beta\psi_b \tag{3.1}$$

$$\psi_s = \beta\psi_r + \alpha\psi_b \tag{3.2}$$

where ψ_r and ψ_b are the zeroth-order repulsive and bound state; ψ_a and ψ_s are the eigenstates formed from antisymmetric and symmetric combinations of these coupled zeroth-order states. The α and β are the coefficients for the mixing states and are expressed as

$$\alpha = \frac{\sqrt{4H_{rb}^2 + \delta^2} + \delta}{2\sqrt{4H_{rb}^2 + \delta^2}} \tag{4.1}$$

$$\beta = \frac{\sqrt{4H_{rb}^2 + \delta^2} - \delta}{2\sqrt{4H_{rb}^2 + \delta^2}} \tag{4.2}$$

where H_{rb} is the matrix element for the coupling and $\delta = E_r - E_b$ is the separation of the unperturbed levels. Because $\Delta E_b/\hbar$ is much smaller than $\Delta E_r/\hbar$, the β term is neglected. Because the selection rule $\Delta J = 0$ allows only levels with the same *J* to couple with each other, the relationship between δ and *J* can be expressed as

$$\delta = E_r - E_b = (\nu_0^r - \nu_0^b) + (B_r - B_b)J(J+1) = C_0 + C_{rb}J(J+1) \tag{5}$$

where ν_0 and *B* are the molecular constants for the repulsive state and the bound state. At the low *J* region, C_0 dominates the coupling strength to affect the predissociation rate. The value of C_0 can be positive or negative depending on whether the centrifugal potential of the repulsive state lies above or below that of the bound state. C_{rb} is negative because B_r should be greater than B_b. Since a decreasing trend with a minimum at $J = 27$ was observed, it is reasonable to assume that $\delta = 0$ at $J = 27$ so for the purpose of estimating the fitting value for C_0 and C_{rb}. Such an assumption results in a positive value for C_0 which implies that the repulsive state lies above the bound state.

There are interactions, such as centrifugal distortion, spin−rotation, rotation−rotation, and Coriolis interactions, which are *J*-dependent couplings. In order to make the couplings more explicit, the basis set for Hund's case (a), $|J\Lambda S\Sigma\Omega\rangle$, is adopted to allow as many as five quantum numbers to describe the molecular rotation. *J* represents the total angular momentum. Λ represents the projection of electronic angular momentum, denoted as *L*, onto the molecular coordinate *z* axis. *S* is the total spin. Σ is the spin component, and $\Omega = \Lambda + \Sigma$. Because the bound state is a singlet state with $S = 0$, it implies that spin rotation interaction makes no contribution to the repulsive-bound coupling H_{rb}. Using these notations, the rotational angular momentum *R* is expressed as

$$R = J - S - L \tag{6}$$

Then $H_{rb} = C_R R^2$ can be expressed as[19]

$$\langle J'\Lambda'S'\Sigma'\Omega'|R^2|J\Lambda S\Sigma\Omega\rangle = C_R\Big\{\delta_{\Sigma'\Sigma}\delta_{\Omega'\Omega}[J(J+1) - \Omega^2 + S(S+1) - \Sigma^2 + \langle L_x^2 + L_y^2\rangle] - 2\sum_{q\pm1}(-1)^{J-\Omega'+S-\Sigma'} \times \begin{bmatrix} J & 1 & J \\ -\Omega' & q & \Omega \end{bmatrix}\begin{bmatrix} S & 1 & S \\ -\Sigma' & q & \Sigma \end{bmatrix} \times [J(J+1)(2J+1)S(S+1)(2S+1)]^{1/2}\Big\} \tag{7}$$

Regarding the *J*-dependence only, we assumed that $\Omega = S = \Sigma = 0$, and the first term becomes $J(J+1)$. Because of the selection rules of predissociation $\Delta J = 0$, $\Delta S = 0$, and $\Delta\Sigma = 0$, the second term is zero. Analogically, the centrifugal distortion can be represented by a second-order polynomial terms of $J(J+1)$ in the H_{rb} expression.

The matrix elements of Coriolis coupling terms of the form J·L in the Hund's case (a) basis set are expressed as

$$\langle J'\Lambda'S'\Sigma'\Omega'|J\cdot L|J\Lambda S\Sigma\Omega\rangle = \delta_{SS'}\delta_{\Sigma\Sigma'}\delta_{JJ'}\sum_q(-1)^{J-\Omega} \times \langle\Lambda'|T_q^1(L)|\Lambda\rangle \times \begin{bmatrix} J & 1 & J \\ -\Omega & q & \Omega' \end{bmatrix}\langle J||T^1(J)||J\rangle \tag{8}$$

where $T_q^1(L)$ and $T^1(J)$ are *J* and *L* in spherical tensor representation, and $\langle J||T^1(J)||J\rangle$ is the reduced matrix.[20] For the case of predissocation, the perpendicular Coriolis interaction that leads to the *J*-dependent coupling strength can be simplified to $J\cdot L \propto \sqrt{J(J+1) - l(l+1)}$.[21,22] Although the above three couplings explicitly give respectively first, second, and one-half orders in $J(J+1)$ for the *J*-dependence, it is not feasible to extract information from the data in Figure 4 for each one by putting all of them into H_{rb}. Instead, the polynomial form of H_{rb} is chosen to be $J(J+1)$. The reasons are given as follows: The second-order term is left out, because it originates

from centrifugal coupling which has a different sign from the first-order term (rotation−rotation coupling). If it were taken, it ought to be a small contribution; otherwise resonance at some J levels would have been observed in Figure 4. The one-half order (Coriolis interaction) is omitted based on the assumption that the 46 482 cm^{-1} band has low vibrational quanta, which probably weakly interacts with rapid vibrational motion of the repulsive state. If it were included, the expression $\sqrt{J(J+1)}$ would approach J as J becomes large and can be included in the $J(J+1)$ expression. It should be noted that, for the present expression of H_{rb}, based on the data of Figure 4 without detailed spectroscopic information of the repulsive potential, it is not feasible to give a clear physical meaning for H_{rb}.

The strength of H_{rb} monotonically increases with J to make the mixing coefficient asymptotically approach 50%. Therefore, no drastic J-dependent predissociation rate shall be observed at high J levels except that a resonance occurs at a particular J level. Nevertheless, an increasing trend with a maximum at $J = 39$ is observed in Figure 4. In order to explain the above observation, a candidate for such J-dependent effect shall have character that the effect is negligible at low, J, but it becomes important at high J. The solution is to consider the lifetime of the repulsive state, expressed as $\hbar/\Delta E_r$ in eq 2, to be J-dependent as well. The relationship between the J-dependent lifetime and the rotational motion in a centrifugal potential is described as follows.

According to Herzberg[23] the effective potential for a rotating system is expressed as

$$U_j(r) = U_0(r) + \frac{h}{8\pi^2 c\mu r^2}J(J+1) \qquad (9)$$

where $U_0(r)$ is the potential for the nonrotating molecule. Unlike $U_0(r)$, the $U_J(r)$ curves for $J > 0$, coming from a large r value, usually first go through a maximum and then through a minimum that corresponds to the equilibrium position. With increasing J, the minimum becomes shallower and finally coincides with the maximum at the point of inflection. As a result, higher J levels no longer have a maximum and a minimum. Such a potential has been graphically depicted by Villars and Condon.[24] Because of the existence of a maximum, the molecule is separated by a high potential barrier from the dissociative state. If a transition were to take place, it would require tunneling through this potential barrier. The transition probability T for this, expressed using the Wentzel−Kramers−Brillouin (WKB) approach is

$$|T|^2 \approx \exp\left(-2\int dr\sqrt{\left(\frac{2m}{\hbar^2}\right)(U_j(r) - E)}\right) \qquad (10)$$

Substituting eq 9 into eq 10

$$|T|^2 \propto \exp(-\sqrt{J(J+1)}) \qquad (11)$$

After expansion

$$|T|^2 \propto 1 + C_{w1}\sqrt{J(J+1)} + C_{w2}J(J+1) \qquad (12)$$

We assume that the J-dependent predissociation rate at high J has a similar J-dependent expression as that of the transition probability. Because this effect appears to become important at $J = 29$, the predissociation rate $U_{J>27}$ is expressed as

$$U_{J>27} = C_{w0} + C_{w1}\sqrt{J(J+1)} + C_{w2}J(J+1) \qquad (13)$$

where C_{w0} is a fitting parameter in which the contribution from δ and H_{rb} can be included. Table 2 lists the best values for the fitting parameters C_0, C_{rb}, C_R, C_{w0}, C_{w1}, and C_{w2}. The results of the fitting are represented by open circles in Figure 4. The fitting values listed in Table 2 indicate that the centrifugal potential of the repulsive state is not significantly different from that of the bound state. Does it imply that because the predissociation taking place is so fast that the rotational characters of the bound state is preserved in the repulsive state? On the basis of only the one case here, it remains inconclusive.

TABLE 2: Values of the Fitting Parameters for the *J*-Dependent Predissociation Rate

separation (δ) $C_0 + C_{rb}J(J+1)$		coupling (H_R) $C_RJ(J+1)$	centrifugal potential ($U_{J>27}$) $C_{w0} + C_{w1}\sqrt{J(J+1)} + C_{w2}J(J+1)$		
C_0[a]	C_{rb}[a]	C_r[a]	C_{w0}[b]	C_{w1}[b]	C_{w2}[b]
0.0012	1.5×10^{-6}	5×10^{-5}	−0.576	0.045	−0.000 59

[a] cm^{-1}. [b] 10^{12}/s.

IV. Conclusion

By using the method of single vibronic level pump−probe fluorescence depletion, we were able to record the rotationally resolved spectra of CS_2 in the energy range from 45 000 to 49 000 cm^{-1}. The band at 46 482 cm^{-1} is particular interesting. Although the molecular constants were derived from the analysis, the assignment of this band's symmetry still needs further investigation.

The observed J-dependent predissociation rate was interpreted by perturbation theory at low J levels and the WKB method at high J levels. The separation of two perturbed states is clearly defined, but the coupling strength has loose physical meaning. The analysis shows no significant difference in the rotational characters between the bound state and the repulsive state.

In addition to our measurement, various methods have been applied to measure the lifetime of the $^1B_2(^1\Sigma_u^+)$ state. Lifetimes of 1.2−9 ps in the range 200−216 nm were reported by fluorescence quantum yield[10], which in general, shown by Mank et al.,[13] are at least a factor of 2 longer than those measured for what appear to be the same bands by the method of the Raman depolarization ratio method.[25,26] The lifetime of 0.6 ps at 205 nm, which is 1 order of magnitude shorter, was measured by femtosecond (1+1) REMPI.[27] In the range 45 100−50 600 cm^{-1}, we have observed that the lifetime changes from band to band. The 46 482 cm^{-1} band with a lifetime of 3−5 ps is a band with the longest lifetime in this range. The lifetime of the band at 47 562 cm^{-1} deduced from band contour simulation was reported to be 4.4 ps by Liou et al.[12] and 2.8 ps by Mank et al.[13] The former was measured at a rotational temperature of 10 K, while the latter was at 30 K. This indicates that the lifetime of the 47 562 cm^{-1} band may be J-dependent as well.

Acknowledgment. The authors thank Dr. A. Kung for his valuable discussions. This research was supported, in part, by the National Science Council, ROC, under Grant NSC 86-2113-M-001-035.

References and Notes

(1) Kleman, B. *Can. J. Phys.* **1963**, *41*, 2034.
(2) Jungen, Ch.; Malm, D. N.; Merer, A. J. *Can. J. Phys.* **1973**, *51*, 1471.
(3) Ochi, N.; Watanabe, H.; Tsuchiya, S. *Chem. Phys.* **1987**, *113*, 271.
(4) Price, W. C.; Simpson, D. M. *Proc. R. Soc. London, Ser. A* **1938**, *165*, 272.
(5) Mulliken, R. S. *Can. J. Chem.* **1958**, *30*, 10.
(6) Walsh, A. D. *J. Chem. Soc.* **1953**, 2267.

(7) Douglas, A. E.; Zanon, I. *Can. J. Phys*. **1964**, *42*, 627.
(8) Greening, F. R.; King, G. W. *J. Mol. Spectrosc*. **1976**, *59*, 312.
(9) Hemley, R. J.; Leopold, D. G.; Roebber, J. L.; Vaida, V. *J. Chem. Phys*. **1983**, *79*, 5219.
(10) Hara, K.; Phillips, D. *Trans. Faraday Soc*. **1978**, *74*, 1441.
(11) Yang, S. C.; Freedman, A.; Kawasaki, M.; Bersohn, R. *J. Chem. Phys*. **1980**, *72*, 4058.
(12) Liou, H. T.; Dan, P.; Hsu, T. Y.; Yang, H.; Lin, H. M. *Chem. Phys. Lett*. **1992**, *192*, 560.
(13) Mank, A.; Starrs, C.; Jego, M. N.; Hepburn, J. W. *J. Chem. Phys*. **1996**, *104*, 3609.
(14) Bernath, P. F.; Dulick, M.; Field, R. W.; Hardwick, J. L. *J. Mol. Spectrosc*. **1981**, *86*, 275.
(15) Liou, H. T.; Yang, H.; Dan, P. *Appl. Phys*. **1992**, *B54*, 221.
(16) Manuscript in preparation.
(17) Liou, H. T.; Dan, P.; Yang, H.; Yuh, J. Y. *Chem. Phys. Lett*. **1991**, *176*, 109.
(18) Minguzzi, P.; Lieto, A. Di. *J. Mol. Spectrosc*. **1985**, *109*, 388.
(19) Brown, J. M.; Kopp, I.; Malmberg, C.; Rydh, B. *Phys. Scr*. **1978**, *17*, 55.
(20) Edmonds, A. R. *Angular Momentum in Quantum Mechanics*; Princeton University Press: Princeton, 1960.
(21) Pine, A. S. In *Structure and Dynamics of Weakly Bound Molecular Complexes*; Weber, A., Ed. Reidel: Dorchecht, 1987; p 93.
(22) Nesbitt, D.; Lascola, R. *J. Chem. Phys*. **1992**, *97*, 8096.
(23) Herzberg, G. *Spectra of Diatomic Molecule*; Van Nostrand Reinhold Company: New York, 1950; p 426.
(24) Villars, D. S.; Condon, E. U. *Phys. Rev*. **1930**, *35*, 1028.
(25) Li, B.; Meyers, A. B. *J. Chem. Phys*. **1988**, *89*, 6658.
(26) Li, B.; Meyers, A. B. *J. Chem. Phys*. **1991**, *94*, 2458.
(27) Baronavski, A. P.; Owrutsky, J. C. *Chem. Phys. Lett*. **1994**, *221*, 419.